

**Probing the Flavor-Changing tc vertex via Tree-Level Processes: $e^+e^- \rightarrow t\bar{c}\nu_e\bar{\nu}_e$, $t\bar{c}e^+e^-$
and $t \rightarrow cW^+W^-$**

S. Bar-Shalom^a, G. Eilam^b, A. Soni^c and J. Wudka^a

^a Physics Dept., University of California, Riverside CA 92521.

^b Physics Dept., Technion-Israel Inst. of Tech., Haifa 32000, Israel.

^c Physics Dept., Brookhaven Nat. Lab., Upton NY 11973, USA.

Abstract

Abstract: The reactions $e^+e^- \rightarrow t\bar{c}\nu_e\bar{\nu}_e$, $t\bar{c}e^+e^-$ are very sensitive probes of the flavor-changing-scalar couplings which can occur in a model with one extra Higgs doublet. At the Next Linear Collider, with a center of mass energy of $\sqrt{s} = 0.5\text{--}2$ TeV, several hundreds and up to thousands of such events may be produced if the mass of the light neutral Higgs is a few hundred GeV. We also briefly comment on the decays $t \rightarrow cW^+W^-$, $t \rightarrow cZZ$. All of these reactions are severely suppressed in the Standard Model.

Understanding the nature of the scalar sector in electroweak theories and searching for flavor-changing (FC) currents are clearly important goals of the next generation of high energy colliders. The purpose of this work is to point out that the reactions:

$$e^+ + e^- \rightarrow t\bar{c}\nu_e\bar{\nu}_e; \bar{t}c\nu_e\bar{\nu}_e; \bar{t}ce^+e^-; \bar{t}ce^+e^- \quad (1)$$

are extremely sensitive probes for such investigations and should be accessible to the next generation of e^+e^- linear colliders (NLC) currently being envisaged [1].

As is well known, though there are stringent experimental constraints against the existence of tree level flavor-changing-scalar (FCS) transitions involving the light quarks [2, 3, 4], analogous constraints involving the top quark are essentially non-existent. In fact, it is natural to imagine that FCS interactions are proportional to the masses of the fermions participating at the vertex [3]; in such a scenario the large top mass makes it much more susceptible to FC transitions. This reasoning has led various authors to stress the importance of searching for tree-level FCS interactions involving the top-quark, especially the top-charm ones [5, 6]. Our study indicates that experimental investigations of the reactions in (1) could be very useful in this regard.

A mild extension of the Standard Model (SM) in which one extra scalar doublet is added, allows for large, tree-level FCS interactions [7]. Therefore, the two Higgs doublet model (2HDM) scalar potential is usually constrained by a discrete symmetry [2] whose only role is to forbid tree-level flavor-changing-scalar-currents. If one does not impose such a discrete symmetry by hand, one arrives at a version of the 2HDM, called Model III, wherein the up-type and the down-type quarks are allowed simultaneously to couple to more than one scalar doublet [7]. The diagonalization of the quark mass matrices does not automatically ensure the diagonalization of the couplings with each single scalar doublet. Both up and down type quarks may then have FC couplings and the corresponding Yukawa Lagrangian in this model is [7, 4]

$$\mathcal{L}_Y^{FC} = \xi_{ij}^U \bar{Q}_{i,L} \tilde{\phi}_2 U_{j,R} + \xi_{ij}^D \bar{Q}_{i,L} \phi_2 D_{j,R} + h.c. , \quad (2)$$

where ϕ_2 denotes the second scalar doublet, $\tilde{\phi}_2 \equiv i\tau_2\phi_2$, Q stands for the quark doublets, and U and D for charge 2/3 and (-1/3) quarks singlets; $i, j = 1, 2, 3$ are the generation indices and ξ are 3×3 matrices parameterizing the strength of FC neutral scalar vertices. The spectrum of the scalar sector in this model consists of two neutral Higgs scalars, denoted as h, H and a pseudoscalar A . In addition, the model has two charged scalars H^\pm .

The experimental constraints can be accommodated simply by imposing a hierarchy among the FC vertices [3] whose strength is correlated to the masses of the participating quarks. We will thus take

$$\xi_{ij}^{U,D} = g_W (\sqrt{m_i m_j} / m_W) \lambda_{ij} . \quad (3)$$

which is often called the Cheng-Sher Ansatz (CSA) [3, 4, 7].

In this scenario all our ignorance regarding the FCS vertices is in the couplings λ_{ij} which are free parameters to be experimentally determined. Assuming for now that they are real, there are six such couplings: $\lambda_{sd}, \lambda_{bs}, \lambda_{bd}, \lambda_{cu}, \lambda_{tu}$ and λ_{tc} . Detailed examination of low energy experimental data, primarily from $\Delta\text{flavor} = 2$ processes, leads to $\lambda_{sd}, \lambda_{bs}, \lambda_{cu} \lesssim 0.1$ [4].

Existing experimental information does not provide any useful constraints on λ_{tc} ; in particular, we may well have $\lambda_{tc} \sim \mathcal{O}(1)$ [8]. In this Letter we will show that if $\lambda_{tc} \sim \mathcal{O}(1)$, experiments on reaction (1) at the NLC can lead to spectacular signatures.

Our study shows that an extremely interesting feature of the reactions in (1) is that (within Model III) the cross-section for these reactions can be much larger than the simple s-channel reaction $e^+e^- \rightarrow t\bar{c}$ (see Atwood *et. al.* in [5]). Indeed $\sigma^{\nu\nu tc} \equiv \sigma(e^+e^- \rightarrow t\bar{c}\nu_e\bar{\nu}_e + \bar{t}c\nu_e\bar{\nu}_e)$ is about two orders of magnitude larger than $\sigma(e^+e^- \rightarrow t\bar{c} + \bar{t}c)$ over a large region of parameter space of Model III; also $\sigma^{eetc} \equiv \sigma(e^+e^- \rightarrow t\bar{c}e^+e^- + \bar{t}ce^+e^-)$ is about one order of magnitude bigger than $\sigma(e^+e^- \rightarrow t\bar{c} + \bar{t}c)$. Moreover, while the cross-section for producing $t\bar{c}$ drops as \sqrt{s} increases, the cross-sections σ^{eetc} and $\sigma^{\nu\nu tc}$ increase with energy in the range $0.5 \text{ TeV} < \sqrt{s} < 2 \text{ TeV}$. Thus, even if no $t\bar{c}$ events are detected at $\sqrt{s} = 0.5 \text{ TeV}$ via $e^+e^- \rightarrow t\bar{c}$, there is still a strong motivation to look for signatures of (1), especially at somewhat higher energies.

In exploring the reactions $e^+e^- \rightarrow t\bar{c}\nu_e\bar{\nu}_e$, $t\bar{c}e^+e^-$ we will use the effective vector boson approximation (EVBA) [9]. The salient features of reaction (1) are then well approximated by the simpler fusion reactions

$$W^+W^-, ZZ \rightarrow t\bar{c}, \bar{t}c \quad (4)$$

The corresponding cross sections for the reactions in (1) are then calculated by folding in the distribution functions $f_{h_V}^V$, for a vector boson V (W or Z) with helicity h_V [10].

The EVBA has been extensively studied in the production of a $t\bar{t}$ pair [11]. There is, however, a significant difference between fusion leading to $t\bar{c}$ and to $t\bar{t}$ primarily due to the appreciable difference in the threshold of the two-reactions, due to $m_t \gg m_c$. For $t\bar{c}$ the fraction of the incoming vector-boson energy, $x = \sqrt{\hat{s}}/s$ (\hat{s} is the c.m. energy squared in the VV c.m. frame and s in the e^+e^- c.m. frame), can drop below 0.05 near threshold, for $\sqrt{s} \gtrsim 0.8 \text{ TeV}$. In this small- x range ($x \lesssim 0.05$) the distribution functions are overestimated within the leading log approximation [11, 12]. We will therefore use the distribution functions which retain higher orders in m_V^2/s as given in Ref. [12]. In the cross section $\sigma(VV \rightarrow t\bar{t})$ the dominant contribution $\propto (m_t/m_V)^4$ is generated by the longitudinal vector-boson contributions for which the polarization vector can be approximated by $\epsilon_0^\mu(k) \simeq k^\mu/m_V$. This approximation does not necessarily hold for the reaction $VV \rightarrow t\bar{c}$ for which $m_V^2/\hat{s} \approx m_V^2/m_t^2$ near threshold. In particular, the cross-section for the reaction $VV \rightarrow \mathcal{H} \rightarrow t\bar{c}$ (\mathcal{H} denotes a neutral Higgs particle) scales like $|\epsilon_{h_{V1}}^{V1} \cdot \epsilon_{h_{V2}}^{V2}|^2$ (see below). Thus not only is the $(m_t/m_V)^4$ factor absent, but also, near threshold, the contribution from the transversely polarized V 's is comparable to that of the longitudinal V 's. We will therefore perform an exact calculation of $\hat{\sigma}(VV \rightarrow \mathcal{H} \rightarrow t\bar{c})$ keeping all possible polarizations of the two colliding vector-bosons.

It is interesting to note that while at tree-level, $\sigma^{eetc} = 0$ in the SM, the parton level reaction $W^+W^- \rightarrow t\bar{c}$ can proceed at tree-level, via Fig. 1a. However, numerically, due to GIM suppression, the results is found to be too small to be of experimental relevance: $\sigma_{\text{SM}}^{\nu\nu tc} \approx 10^{-5} - 10^{-4} \text{ fb}$ for $\sqrt{s} = 0.5 - 2 \text{ TeV}$ [13]. We will henceforth neglect the SM contribution.

In Model III there is an additional important tree-level contribution (see Fig. 1b), originating from $VV \rightarrow \mathcal{H} \rightarrow t\bar{c}, \bar{t}c$. Choosing for simplicity $\lambda_{tc} = \lambda_{ct} = \lambda_R + i\lambda_I$, the relevant terms of the

Model III Lagrangian with the CSA become:

$$\mathcal{L}_{\mathcal{H}tc} = -\frac{g_W}{\sqrt{2}} \frac{\sqrt{m_t m_c}}{m_W} f_{\mathcal{H}} \mathcal{H} \bar{t}(\lambda_R + i\lambda_I \gamma_5) c, \quad (5)$$

$$\mathcal{L}_{\mathcal{H}VV} = -g_W m_W C_V c_{\mathcal{H}} \mathcal{H} g_{\mu\nu} V^\mu V^\nu, \quad (6)$$

where $C_{W;Z} = 1; m_Z^2/m_W^2$, $f_{h;H} \equiv \cos \tilde{\alpha}; \sin \tilde{\alpha}$ and $c_{h;H} \equiv \sin \tilde{\alpha}; -\cos \tilde{\alpha}$. The mixing angle $\tilde{\alpha}$ is determined by the Higgs potential. Note that the pseudoscalar A does not couple to gauge bosons and is therefore irrelevant for the reactions at hand.

Within Model III $\sigma^{\nu tc}, \sigma^{etc}(\tilde{\alpha} \rightarrow 0 \text{ or } \pi/2) \rightarrow 0$ at the tree-level. For definiteness, we will present our numerical results for $\tilde{\alpha} = \pi/4$ [13, 14]. In calculating the cross sections we vary the mass of the lighter scalar h in the range $0.1 \text{ TeV} < m_h < 1 \text{ TeV}$, while holding fixed the mass of the heavy scalar H at $m_H = 1 \text{ TeV}$.

For Model III, $VV \rightarrow t\bar{c}$ proceeds at tree-level via the s-channel neutral Higgs exchange of Fig. 1b. Neglecting the SM diagram, the corresponding parton-level cross-section $\hat{\sigma}_V \equiv \hat{\sigma}(V_{h_{V1}}^1 V_{h_{V2}}^2 \rightarrow t\bar{c})$ is given by:

$$\hat{\sigma}_V = \frac{(\sin 2\tilde{\alpha})^2 N_c \pi \alpha^2}{4\hat{s}\beta_V s_W^4} \left(\frac{m_V}{m_W}\right)^4 |\epsilon_{h_{V1}}^{V1} \cdot \epsilon_{h_{V2}}^{V2}|^2 |\Pi_h - \Pi_H|^2 \times \sqrt{\Delta_t \Delta_c a_+ a_-} (a_+ \lambda_R^2 + a_- \lambda_I^2), \quad (7)$$

where $\Delta_\ell = m_\ell^2/\hat{s}$, $a_\pm = 1 - (\sqrt{\Delta_t} \pm \sqrt{\Delta_c})^2$, $\beta_\ell \equiv \sqrt{1 - 4\Delta_\ell^2}$ and

$$\Pi_{\mathcal{H}} = \left(1 - \Delta_{\mathcal{H}}^2 + i\Delta_{\mathcal{H}}\Delta_{\Gamma_{\mathcal{H}}}\right)^{-1}, \quad \Delta_{\Gamma_{\mathcal{H}}}^2 \equiv \Gamma_{\mathcal{H}}^2/\hat{s}. \quad (8)$$

Given the couplings of Model III, the width of \mathcal{H} ($\Gamma_{\mathcal{H}}$) can be readily calculated [15]. The leading decay rates in this model are $\mathcal{H} \rightarrow b\bar{b}, t\bar{t}, ZZ, W^+W^-$ and $t\bar{c}, c\bar{t}$. We include all these contributions when calculating the above cross-sections. In our numerical results we will ignore CP violation and take $\lambda_I = 0$ and set $\lambda_R = \lambda$.

Due to the orthogonality properties of the polarization vectors of the two spin one bosons there is no interference between the transverse and the longitudinal polarizations. Note that $|\epsilon_{\pm}^{V1} \cdot \epsilon_{\mp}^{V2}|^2 = 0$, $|\epsilon_{\pm}^{V1} \cdot \epsilon_{\pm}^{V2}|^2 = 1$, and $|\epsilon_0^{V1} \cdot \epsilon_0^{V2}|^2 = (1 + \beta_V^2)/(1 - \beta_V^2)^2$ which grows with \hat{s} . However, we can see from (7), that $\hat{\sigma}_V(\Delta_{\mathcal{H}} \rightarrow 0) \rightarrow 0$ ensuring unitarity of the hard cross-section.

In general, the transverse distribution functions are bigger than the longitudinal ones for $x \gtrsim 0.1$ [11, 12]. Therefore, the relative smallness of the transverse hard cross-section compared to the longitudinal one is partly compensated for in the full cross-section. In particular, we find that the contribution from the transversely polarized W 's (Z 's) can give at most 25%(35%) of the corresponding full cross-section $\sigma^{\nu tc}(\sigma^{etc})$.

It is evident from (7) that neglecting the small difference between m_W and m_Z one finds $\hat{\sigma}_W = \hat{\sigma}_Z$. The main difference between $\sigma^{\nu tc}$ and σ^{etc} arises from the dissimilarity between the distribution functions for W and Z bosons. In particular, disregarding the subleading transverse

parts of the WW and the ZZ cross-sections, the relative strength between the W and the Z longitudinal distribution functions is given by [11, 12]:

$$f_0^Z = 2c_W^{-2} (2s_W^4 - s_W^2 + 1/4) f_0^W \approx f_0^W/3 , \quad (9)$$

Therefore, since the cross-sections $\sigma^{\nu tc}$ and σ^{etc} are dominated by collisions of longitudinal W 's and Z 's, respectively, σ^{etc} is expected to be smaller by about one order of magnitude than $\sigma^{\nu tc}$, which is indeed what we find. We will thus only present numerical results for $\sigma^{\nu tc}$, keeping in mind that σ^{etc} exhibits the same behavior though suppressed by about one order of magnitude.

Fig. 2 shows the dependence of the scaled cross-section $\sigma^{\nu tc}/\lambda^2$ on the mass of the light Higgs m_h for four values of s [16]. The cross-section peaks at $m_h \simeq 250$ GeV and drops as the mass of the light Higgs approaches that of the heavy Higgs. Indeed as $m_h \rightarrow m_H$, $\sigma^{\nu tc}/\lambda^2 \rightarrow 0$ as expected when $\tilde{\alpha} = \pi/4$ for which the couplings htc and Htc are identical. However, this ‘‘GIM like’’ cancelation does not operate when $\tilde{\alpha} \neq \pi/4$ for which $\sigma^{\nu tc}/\lambda^2$ can stay at the fb level even for $m_h \rightarrow m_H$ [13]. When $\sqrt{s} = 2$ TeV the cross-section is about 5 fb for $\lambda = 1$ and $m_h \approx 250$ GeV. Note that the cross-section scales like λ^2 so that even a moderate change of λ , say by a factor of three, can increase or decrease the cross-section by one order of magnitude.

It is evident from Fig. 2 that, for $m_h \simeq 250$ GeV, in a NLC running at $\sqrt{s} \gtrsim 1$ TeV with an integrated luminosity of $\mathcal{L} \gtrsim 10^2$ [fb] $^{-1}$, Model III (with $\lambda = 1$) predicts hundreds and up to thousands of $t\bar{c}\nu_e\bar{\nu}_e$ events, and tens to hundreds of $t\bar{c}e^+e^-$ events. Note also that even with $m_h \approx 500$ GeV, this projected luminosity can yield hundreds of $t\bar{c}\nu_e\bar{\nu}_e$ events and tens of $t\bar{c}e^+e^-$ events at $\sqrt{s} = 1.5$ TeV. The corresponding SM prediction is of course essentially zero events.

It is also instructive to compare in Model III the production rate of $e^+e^- \rightarrow t\bar{c}\nu_e\bar{\nu}_e$ with that of $e^+e^- \rightarrow t\bar{t}\nu_e\bar{\nu}_e$. We recall that $\sigma^{\nu tt} \equiv \sigma(e^+e^- \rightarrow W^+W^-\nu_e\bar{\nu}_e \rightarrow t\bar{t}\nu_e\bar{\nu}_e)$ is dominated by collisions of two longitudinal W 's at the parton level [11]. The reaction $W^+W^- \rightarrow t\bar{t}$ can proceed through the t -channel b quark exchange and the s -channel γ, Z, h and H exchanges (the diagrammatic description can be found in [11, 17]). The helicity amplitudes for $W_L^+W_L^- \rightarrow t\bar{t}$ are:

$$\begin{aligned} \mathcal{A}_{\eta=\bar{\eta}} &= \frac{\pi\alpha}{s_W^2} \frac{m_t\sqrt{s}}{m_W^2} \left(\left[\frac{(1+\beta_t^2)\cos\theta-2\beta_t}{1+\beta_t^2-2\beta_t\cos\theta} \right] - \sum_{\mathcal{H}=h,H} \beta_t c_{\mathcal{H}} b_{\mathcal{H}} \Pi_{\mathcal{H}} \right) \\ \mathcal{A}_{\eta=-\bar{\eta}} &= \frac{2\pi\alpha}{s_W^2} \frac{m_t^2}{m_W^2} \left(\frac{\eta+\beta_t}{1+\beta_t^2-2\beta_t\cos\theta} \right) \sin\theta , \end{aligned} \quad (10)$$

where η and $\bar{\eta}$ denote the helicities of the t and \bar{t} quarks respectively, $b_{(h;H)} = (-\sin\tilde{\alpha} + u\cos\tilde{\alpha}; \cos\tilde{\alpha} + u\sin\tilde{\alpha})$, $u = \sqrt{2}(\lambda_R - i\eta\lambda_I/\beta_t)$; θ is the CM scattering angle, and $c_{\mathcal{H}}$ is given in (6) [18]. For simplicity we assumed $\lambda_{tt} = \lambda_{tc} = \lambda$.

In Fig. 3 we plot the ratio $R^{tc/tt} \equiv \sigma^{\nu tc}/\sigma^{\nu tt}$ within Model III, for $\lambda = 1$, $\tilde{\alpha} = \pi/4$ and $m_H = 1$ TeV as a function of the light Higgs mass, m_h , and for $\sqrt{s} = 0.5, 1, 1.5$ and 2 TeV. We find that $\sigma^{\nu tt}$ depends very weakly on m_h , with a small peak at around $m_h = 400$ GeV which fades as \sqrt{s} grows. For $\sqrt{s} = 0.5$ TeV and in the range $200 \text{ GeV} \lesssim m_h \lesssim 400 \text{ GeV}$, $R^{tc/tt} > 1$. In particular, for $m_h \approx 250$ GeV, $\sigma^{\nu tc}$ can become almost two orders of magnitude larger than

$\sigma^{\nu vt}$. As \sqrt{s} grows, $R^{tc/tt}$ drops; in the range $200 \text{ GeV} \lesssim m_h \lesssim 400 \text{ GeV}$, we find that for $\sqrt{s} = 1 \text{ TeV}$, $R^{tc/tt} > 0.1$, while for $\sqrt{s} = 1.5 - 2 \text{ TeV}$, $0.01 \lesssim R^{tc/tt} \lesssim 0.1$.

The dependence of $\sigma^{\nu vt}$ on λ is significant only near its peak (at $m_h \sim 400 \text{ GeV}$); for $200 \text{ GeV} \lesssim m_h \lesssim 400 \text{ GeV}$, where $R^{tc/tt}$ acquires its largest values, $R^{tc/tt}$ roughly scales as λ^2 . Thus, again even a mild change in λ can alter $R^{tc/tt}$ appreciably. Hence, within Model III, with m_h in the few-hundred GeV range, it is possible to observe comparable production rates for the $t\bar{c}\nu_e\bar{\nu}_e$ and $t\bar{t}\nu_e\bar{\nu}_e$ even at a NLC running at CM energies of about a TeV.

Next we discuss the two rare decays $t \rightarrow W^+W^-c$ and $t \rightarrow ZZc$. The latter is, of course, possible only if $m_t > 2m_Z + m_c$. Within the SM these decay channels are vanishingly small. For the first one, the tree-level decay, $\text{Br}(t \rightarrow W^+W^-c) \approx 10^{-13} - 10^{-12}$ due to GIM suppression [19, 20]. For the second decay the branching ratio is even smaller since it occurs only at one loop.

The situation is completely different in Model III where both decays occur at the tree-level through the FC Higgs exchange of Fig. 1b. These decays are related to the fusion reactions ($WW, ZZ \rightarrow \bar{t}c$) by crossing symmetry. Thus in terms of the hard cross-section given in (7):

$$\Gamma_V = \frac{m_t^3}{32N_c\pi^2} \int_{4\zeta_V^2}^{(1-\zeta_c)^2} dz z(z - 4\zeta_V^2) \sum_{h_{V1}, h_{V2}} \hat{\sigma}_V|_{\hat{s}=m_t^2 z} \quad (11)$$

where $\Gamma_V \equiv \Gamma(t \rightarrow VVc)$ and $\zeta_\ell \equiv m_\ell/m_t$. The scaled-branching-ratio (SBR) $\text{Br}(t \rightarrow W^+W^-c)/\lambda^2$ is given in Fig. 4; it is largest for $2m_W \lesssim m_h \lesssim m_t$ and drops rapidly in the regions $m_h < 2m_W$ or $m_h > 200 \text{ GeV}$. For a wide range of m_h , the SBR is many orders of magnitude bigger than the SM. Indeed for optimal values of m_h , lying in the very narrow window, $2m_W \lesssim m_h \lesssim m_t$, the SBR $\sim 10^{-4}$. It is typically a few times 10^{-7} for $m_h \gtrsim m_t$ and can reach $\sim 10^{-6}$ in the $m_h \lesssim 2m_W$ region. Concerning $t \rightarrow ZZc$, the branching ratio is typically $\sim 10^{-5}$ for $(2m_Z + m_c) < m_t < 200 \text{ GeV}$ if again m_h lies in a very narrow window, $2m_Z < m_h < m_t$. Note that, in contrast to the SM, within Model III, $\text{Br}(h \rightarrow WW) \sim 1$ for $\tilde{\alpha} = \pi/4$; and, even for $m_h > 2m_t$, $\text{Br}(h \rightarrow WW) \sim 0.7 \gg \text{Br}(h \rightarrow t\bar{t})$ [21]. Both decays are thus very sensitive to m_t : for $170 \text{ GeV} < m_t < 200 \text{ GeV}$, a $\sim 15 \text{ GeV}$ shift in m_t can generate an order of magnitude change in the Br in the region $2m_V < m_h < m_t$.

To summarize, in this paper, we have emphasized the importance of searching for the FC reactions, $e^+e^- \rightarrow t\bar{c}\nu_e\bar{\nu}_e$ and $e^+e^- \rightarrow t\bar{c}e^+e^-$, in a high energy e^+e^- collider. These reactions are sensitive indicators of physics beyond the SM with new FC couplings of the top quark. As an illustrative example we have considered the consequences of extending the scalar sector of the SM with a second scalar doublet such that new FC couplings occur at the tree-level. We found that within a large portion of the free parameter space of the FC 2HDM, these new FC couplings may give rise to appreciable production rates for the $t\bar{c}\nu_e\bar{\nu}_e$ and $t\bar{c}e^+e^-$ final states which can unambiguously indicate the existence of new physics. From the experimental point of view, it should be emphasized that although σ^{eetc} is one order of magnitude smaller than $\sigma^{\nu vt}$, the $t\bar{c}e^+e^-$ signature may be easier to detect as it does not have the missing energy associated with the two neutrinos in the $t\bar{c}\nu_e\bar{\nu}_e$ final state.

In closing, we also wish to remark that it is most likely that the Higgs particle will have been discovered by the time the NLC starts its first run. If indeed such a particle is detected with a mass of a few hundreds GeV, it will be extremely important to investigate the reactions $e^+e^- \rightarrow t\bar{c}\nu_e\bar{\nu}_e$ and $e^+e^- \rightarrow t\bar{c}e^+e^-$ at the NLC as it may serve as a strong evidence for the existence of a non-minimal scalar sector with FC scalar couplings to fermions. In addition, since supersymmetry strongly disfavors $m_h \gtrsim 200$ GeV, the detection of this particle above this limit would encourage the study of a general, non-supersymmetric, extended scalar sector.

We are grateful to David Atwood, Keisuke Fujii, Daniel Wyler and Marc Sher for discussions. We acknowledge partial support from U.S. Israel B.S.F. (G.E. and A.S.) and from the U.S. DOE contract numbers DE-AC02-76CH00016(BNL), DE-FG03-94ER40837(UCR). G.E. thanks the Israel Science Foundation and the Fund for the Promotion of Research at the Technion for partial support.

References

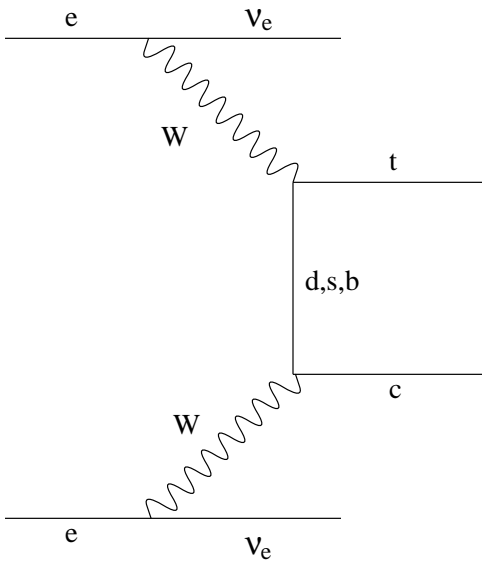
- [1] Proceedings of the Workshop on Physics and Experiments with Linear e^+e^- Colliders, eds. F. Harris *et. al.* World Scientific, Singapore, 1993; A. Miyamoto and Y. Fujii, *ibid*, 1996.
- [2] S. Glashow and S. Weinberg, Phys. Rev. **D15**, 1958 (1977).
- [3] T.P. Cheng and M. Sher, Phys. Rev. **D35**, 3484 (1987); M. Sher and Y. Yuan, Phys. Rev. **D44**, 1461 (1991).
- [4] D. Atwood, L. Reina and A. Soni, hep-ph-9609279.
- [5] M.J. Savage, Phys. Lett. **B266**, 135 (1991); W.S. Hou, Phys. Lett. **B296**, 179 (1992); M. Luke and M.J. Savage, Phys. Lett. **B307**, 387 (1993); L.J. Hall and S. Weinberg, Phys. Rev. **D48**, R979 (1993); D. Atwood *et. al.*, Phys. Rev. **D53**, 1199 (1996).
- [6] W.-S. Hou and G.-L. Lin, Phys. Lett. **B379**, 261 (1996).
- [7] Luke and Savage in Ref. 5.
- [8] λ_{tu} is also not well constrained from existing experiments. The Cheng and Sher Ansatz (3) does, of course, imply a much smaller tu coupling compared to the tc one due to the up-charm mass difference.
- [9] R. Cahn and S. Dawson, Phys. Lett. **B136**, 196 (1984); **136B**, 464(E) (1984); M. Chanowitz and M.K. Gaillard, Phys. Lett. **B142**, 85 (1984); G.L. Kane *et. al.*, Phys. Lett. **B148**, 367 (1984).
- [10] We will use the generic notation V for a vector boson i.e., W^+ , W^- or Z ; in most instances the appropriate choice can be fixed by inspection.
- [11] See e.g., O.J.P. Eboli *et. al.*, Phys. Rev. **D34**, 771 (1986); C.-P. Yuan, Nucl. Phys. **B310**, 1 (1988); R.P. Kauffman, Phys. Rev. **D41**, 3343 (1990).

- [12] See e.g., S. Dawson, Nucl. Phys. **B249**, 42 (1985); P.W. Johnson *et. al.*, Phys. Rev. **D36**, 291 (1987).
- [13] For further details see S. Bar-Shalom *et. al.* (in preparation).
- [14] The cross-section can actually be bigger by about a factor of 3/2 for an optimal choice of $\tilde{\alpha} \approx \pi/6$.
- [15] D. Atwood *et. al.*, Phys. Rev. Lett. **75**, 3800 (1995).
- [16] Note that the scaled cross-section (e.g., $\sigma^{\nu\nu tc}/\lambda^2$) has a residual mild dependence on λ due to the width of the h .
- [17] D. Atwood and A. Soni, hep-ph/9607481.
- [18] In the SM limit, $\tilde{\alpha} = -\pi/4$ and $\lambda_R, \lambda_I = 0$, the hard cross-section for $W_L^+ W_L^- \rightarrow t\bar{t}$, obtained from (10) agrees with the one obtained by Eboli *et. al.* in [11].
- [19] E. Jenkins, preprint, hep-ph-9612211.
- [20] D. Atwood and M. Sher (private communication).
- [21] Note that Hou's analytical results in Ref. 5 correspond to the choice $\tilde{\alpha} = 0$ in our notation. In this special case Higgs decays to WW , ZZ are suppressed at tree level even when $m_H > 2m_W$. In contrast, for illustrative purposes, we are using $\tilde{\alpha} = \pi/4$ in which case $h \rightarrow WW$ becomes the dominant decay.

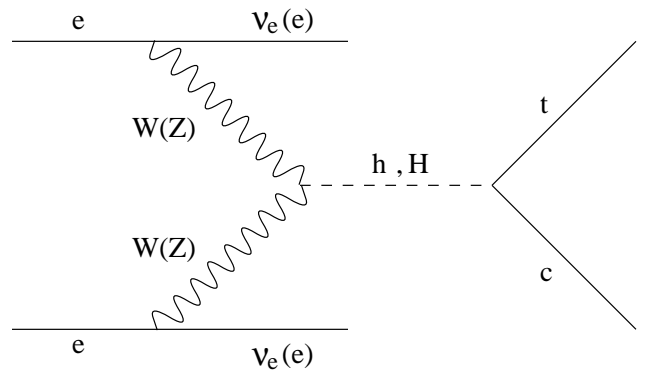
Figure Captions

- Fig. 1: (a) The Standard Model diagram for $e^+e^- \rightarrow t\bar{c}\nu_e\bar{\nu}_e$; (b) Diagrams for $e^+e^- \rightarrow t\bar{c}\nu_e\bar{\nu}_e(e^+e^-)$ in Model III.
- Fig. 2: The cross-section $\sigma(e^+e^- \rightarrow t\bar{c}\nu_e\bar{\nu}_e + \bar{t}c\nu_e\bar{\nu}_e)$ in units of λ^2 as a function of m_h for $\sqrt{s} = 0.5, 1, 1.5$ and 2 TeV.
- Fig. 3: The ratio $R^{tc/tt}$ for $\lambda = 1$ and $m_H = 1$ TeV, as a function of m_h for $\sqrt{s} = 0.5, 1, 1.5$ and 2 TeV.
- Fig. 4: The scaled branching ratio, $Br(t \rightarrow W^+W^-c)/\lambda^2$ as a function of m_h for various values of m_t .

Figure 1



(a)



(b)

Figure 2

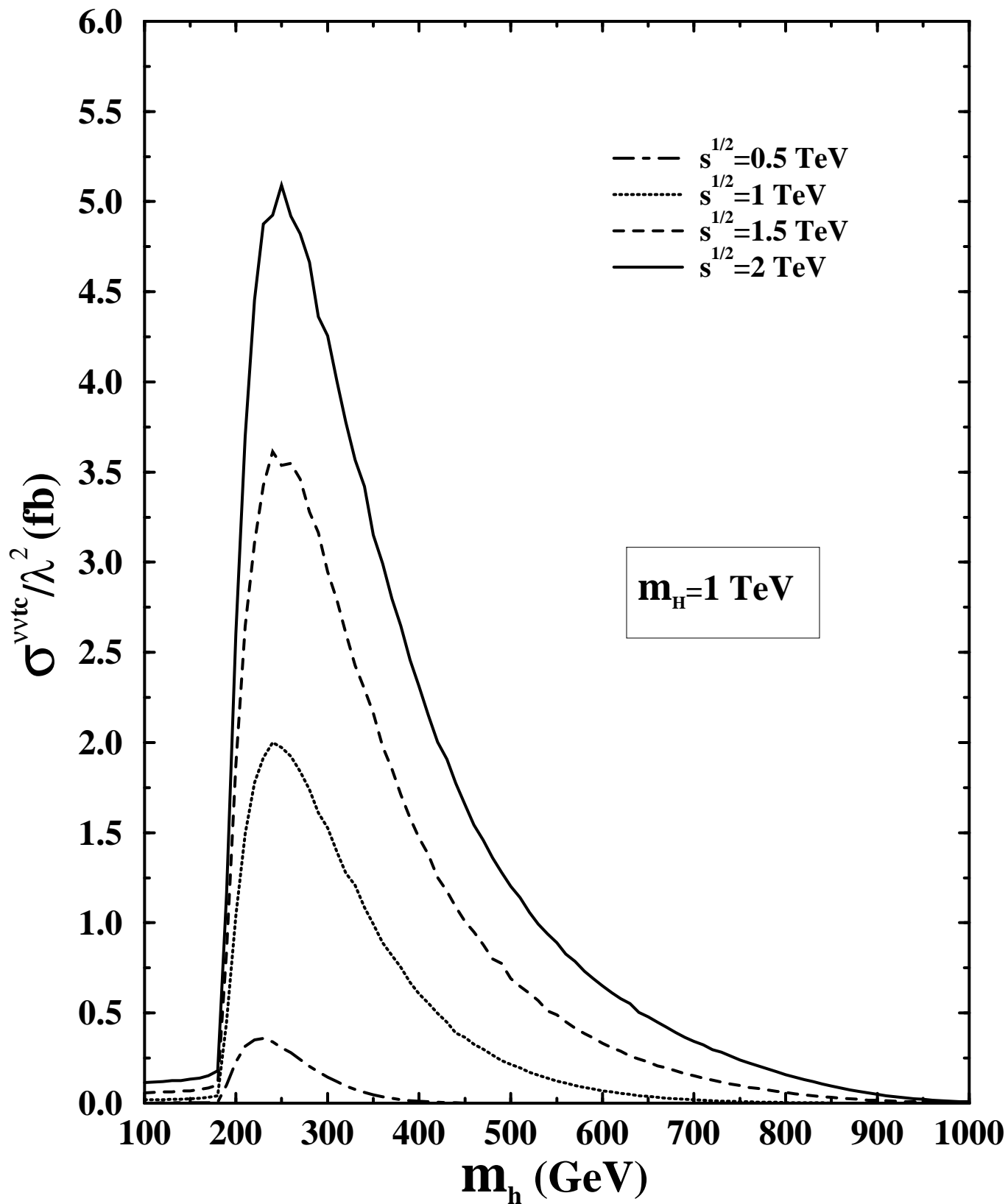


Figure 3

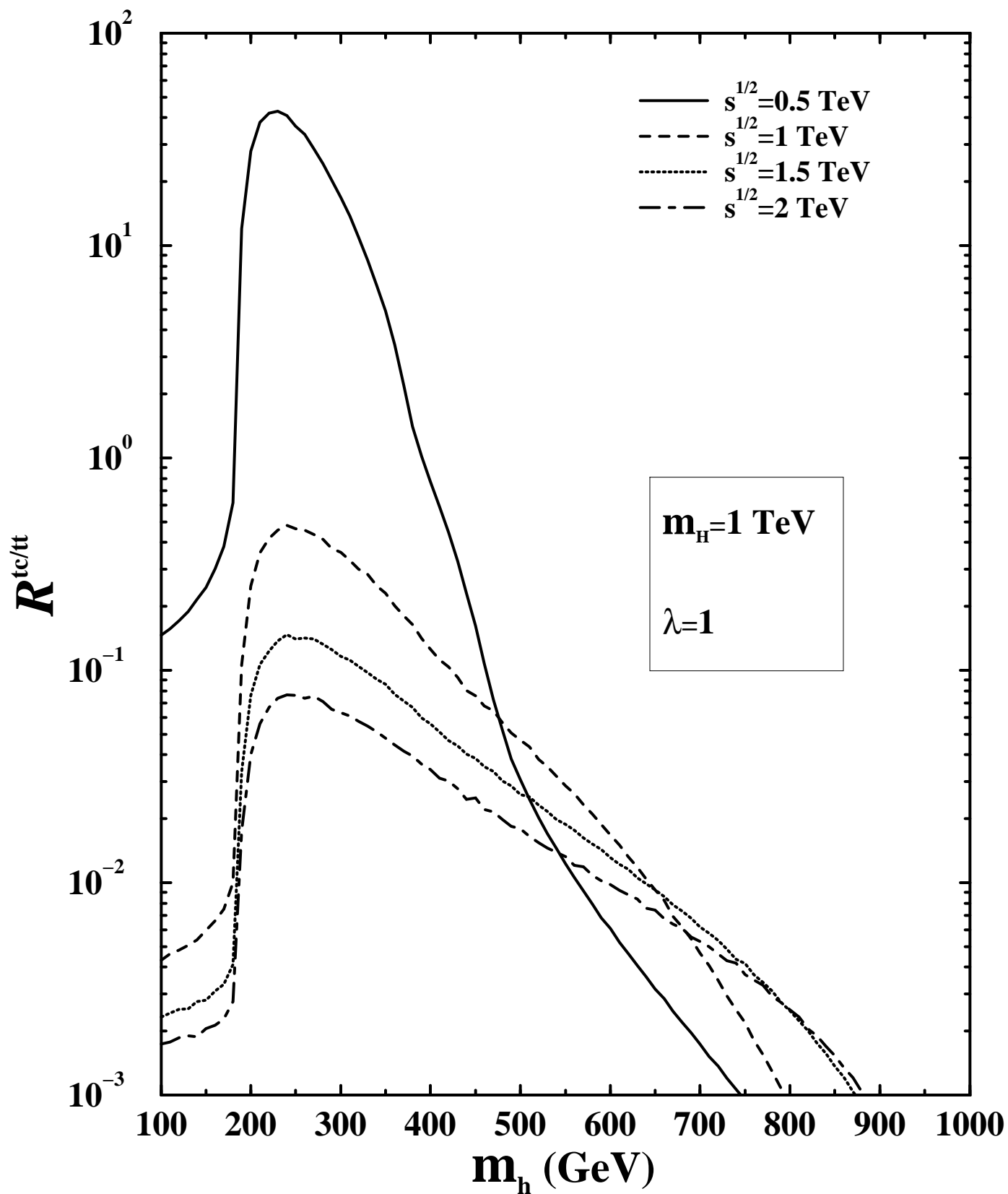


Figure 4

